Dieses Dokument ist eine Zweitveröffentlichung (Postprint Version) /

This is a self-archiving document (accepted version):

Phil Goldberg, Sabine Apelt, Dirk Spitzner, Richard Boucher, Erik Mehner, Hartmut Stöcker, Dirk C.Meyer, Annegret Benke, Ute Bergmann

Icing temperature measurements of water on pyroelectric single crystals: Impact of experimental methods on the degree of supercooling

Diese Version ist verfügbar / This version is available on:

https://nbn-resolving.org/urn:nbn:de:bsz:14-qucosa2-234145

SLUB
Wir führen Wissen.

TECHNISCHE UNIVERSITÄT DRESDEN

Qucosa
Quality Content of Saxony

Accepted Manuscript

Icing Temperature Measurements of Water on Pyroelectric Single Crystals: Impact of Experimental Methods on the Degree of Supercooling

Phil Goldberg, Sabine Apelt, Dirk Spitzner, Richard Boucher, Erik Mehner, Hartmut Stöcker, Dirk C. Meyer, Annegret Benke, Ute Bergmann

Please cite this article as: Goldberg, Phil, Apelt, Sabine, Spitzner, Dirk, Boucher, Richard, Mehner, Erik, Stöcker, Hartmut, Meyer, Dirk C., Benke, Annegret, Bergmann, Ute, Icing Temperature Measurements of Water on Pyroelectric Single Crystals: Impact of Experimental Methods on the Degree of Supercooling, *Cold Regions Science and Technology* (2018), doi:10.1016/j.coldregions.2018.02.008

This is a PDF file of an unedited manuscript that has been accepted for publication. As a service to our customers we are providing this early version of the manuscript. The manuscript will undergo copyediting, typesetting, and review of the resulting proof before it is published in its final form. Please note that during the production process errors may be discovered which could affect the content, and all legal disclaimers that apply to the journal pertain.

Icing Temperature Measurements of Water on Pyroelectric Single Crystals:
Impact of Experimental Methods on the Degree of Supercooling

Phil Goldberg[a],[*], Sabine Apelt[a], Dirk Spitzner[a], Richard Boucher[a], Erik Mehner[b], Hartmut Stöcker[b], Dirk C. Meyer[b], Annegret Benke[a], Ute Bergmann[a]

[a]*Institute for Materials Science and Max Bergmann Center for Biomaterials, TU Dresden, 01062 Dresden, Germany*
[b]*Institute of Experimental Physics, TU Bergakademie Freiberg, Leipziger Straße 23, 09596 Freiberg, Germany*

Abstract

In our experiments, the icing temperature of small water volumes placed on different pyroelectric single crystals ($Sr_xBa_{1-x}Nb_2O_6$, $LiNbO_3$, and $LiTaO_3$) was determined using two measurement setups: (1) the sessile droplet and (2) ring system method. In the first method, a free-standing water droplet was exposed to several external factors in the air environment. This was found to lead to higher icing temperatures compared to the second method where the water was more isolated from external factors such as evaporation. In the second method, the material of the ring system was found to be an important factor determining the freezing temperature of the enclosed water. A recommendation for the application of both methods is given, their advantages and disadvantages depending on the purpose of measurement, and their

---

[*]Corresponding author
Email address: `phil.goldberg@nano.tu-dresden.de` (Phil Goldberg)

reproducibility for practical applications. In addition to this, the correlation between pyroelectricity and icing temperature, with regard to several types of internal and external factors affecting water freezing, is also discussed in the paper.

Keywords: Phase transitions at surfaces and interfaces, crystallization, Pyroelectric effects

PACS: 68.35.Rh, 64.70.dg, 77.70.+a,

1. Introduction

Below the freezing point, water on the surface of a solid material will undergo a phase transformation from the liquid to the solid phase. Water freezing, not only in arctic regions, can have a negative influence on the service-led economy due to the influence of ice accretion on power supply and transport systems. In turn this leads to a reduction of their energy efficiency or even operational breakdown as well as potential safety risks for people. Several widely used strategies have been developed to remove ice, these include electro-thermal treatment, mechanical scraping, and the use of chemical de-icing [Laforte et al., 1998; Frankenstein and Tuthill, 2002]. However, they have many disadvantages: a substantially large amount of energy is needed to clear away the ice and the possible negative environmental impact of chemical de-icing solutions is currently under debate. Contrary to conventional ice removal, preventive anti-icing methods involve surface treatments, which can repel impacting water droplets before they freeze or delay heterogeneous ice nucleation [Saito et al., 1997; Mishchenko et al., 2010]. These passive methods rely on the development of novel surface coatings

2

with chemical and physical properties that prevent ice formation or enable the removal of ice layers with little effort. It is hoped that they will gain industrial attention as a cheap and environment-friendly option.

Novel surface coatings based on the pyroelectric effect are interesting candidates for the prevention/delay of ice formation. Pyroelectric materials exhibit a change in their spontaneous polarization and a corresponding surface charge alternation during a temperature variation due to the associated pyroelectric coefficient. In the case of pyroelectric single crystals, e.g. $LiNbO_3$, $LiTaO_3$, or $BaTiO_3$, the internal polarization is compensated by screening charges from out of the local environment on the surfaces perpendicular to the polar axis until an electrostatic equilibrium is reached. Only when the temperature changes, the surface charge variation can result in a measurable pyroelectric current [Lang, 2005]. The surface charges are responsible for an electric field which can affect the behavior of water molecules in the surrounding. Consequently, it is expected that the pyroelectric effect has an influence on the formation of the hydrogen bond network of supercooled water below its freezing point. Ehre *et al.* have experimentally shown different freezing behavior on positively and negatively charged surfaces of pyroelectric materials [Ehre et al., 2010]. They observed that positively charged surfaces promote ice nucleation, whereas negatively charged surfaces reduce the freezing temperature. In the latter case ice nucleation starts at the air/water interface of the droplet due to the retardation of the heterogeneous nucleation at the solid/water interface. The authors link this delayed ice nucleation on the negatively charged surface to the influence of the surface charge on the water structure at the solid/liquid interface (het-

3

erogeneous nucleation), which is in contrast to homogeneous ice nucleation initiated by an electric field inside the water droplet. Similarly, pyroelectric polyvinylidene fluoride-trifluoroethylene P(VDF-TrFE) copolymer has been shown to cause a remarkable reduction of the icing temperature compared to uncoated glass [Spitzner et al., 2015]. This icing temperature reduction was observed to depend on the polarity of the electric field applied during the thermal treatment of the P(VDF-TrFE). Moreover, the switchable freezing behavior of water under an increasing number of thermal cycles showed a slight training effect which was influenced by with the polarization direction.

The heterogeneous freezing of water droplets has been studied by research groups all over the world with the help of several different types of instruments. The most widely used method is the visual observation of the freezing event. For this, defined volumes of water placed as separated droplets (of 50 to 100 μm sometimes even more than 1 mm in diameter) onto a substrate were investigated with an optical microscope during the freezing on a cooling stage in a chamber system [Zobrist et al., 2007; Nitsch, 2009]. Another option is the usage of a differential scanning calorimeter (DSC), where the nucleation is detected by the release of latent heat during freezing [O'Neill, 1964; Parody-Morreale et al., 1986; Zobrist et al., 2007]. A relatively simple experimental setup consisting of a smooth plate with a good thermal conductivity that is placed in a polystyrene box filled with liquid nitrogen, so that the plate is cooled to a temperature between 200 K and 250 K, and the freezing process of a water droplet was investigated [Snoeijer and Brunet, 2012]. In other experiments, an acrylic glass enclosure was laid over the cold plate and pure nitrogen gas was constantly purged into the enclosure in or-

4

der to isolate the water droplet from humid air and to prevent any water vapor condensing on the droplet [Wang et al., 2006; Singh and Singh, 2013]. Experiments have also been made in which water droplets were immersed in an immiscible medium (suspension method) [Bigg, 1953; Wood and Walton, 1970; Ning and Liu, 2002; Shaw et al., 2005] or were covered with a protective oil film [Carte, 1956] in order to minimize the effects of the container wall and foreign particles and to prevent direct influence of the air environment on ice nucleation. Another way to minimize evaporation is to enclose the water volume by either an O-ring [Seeley and Seidler, 2001] or a thin glass [Shaw et al., 2005]. Several authors carried out their experimental investigation with small water droplets that were condensed from the vapor phase onto a cold surface (droplets of different sizes) [Na and Webb, 2003; Ehre et al., 2010; Li et al., 2012; Oberli et al., 2014; Petit and Bonaccurso, 2014]. Na *et al.* have investigated frost formation by using a low temperature wind tunnel in order to control the air humidity for dropwise condensation on a cold test surface [Na and Webb, 2003].

Droplet-nucleation tests cannot provide a reliable evaluation of the icing temperature due to the coalescence of droplets of various sizes and possible in-plane growth of ice-bridges that propagate across the surface in a chain reaction [Meakin, 1992; Dooley, 2010; Boreyko and Collier, 2013; Guadarrama-Cetina et al., 2013]. Several authors have suggested that the nucleation rate of a sessile droplet depends on its volume, where it is supposed to increase with larger droplet volumes due to the larger number of active nucleating sites, i.e. the freezing temperature is reduced if the water droplet volume decreases [Hoffer, 1961; Pruppacher and Klett, 1978; Zhang et al., 2016].

5

Contrastingly, it was found by Earle *et al.* and Kuhn *et al.* that the rate co-efficient increases with decreasing droplet size for a given temperature as the contribution of surface nucleation appears to increase due to the associated higher surface-to-volume ratio [Earle et al., 2010; Kuhn et al., 2011; O and Wood, 2016]. However, this is only valid for all micrometer-sized supercooled droplets below a droplet size threshold (of few μm) for the case of surface nucleation [Duft and Leisner, 2004].

As part of the freezing experiments on pyroelectric single crystals conducted by Ehre *et al.* droplet condensation took place on the cooled single crystals from humid air. As a consequence of the droplet size dependence of the freezing process it is difficult to definitely correlate the observed differences in the freezing behavior with the polarity of a crystal as Ehre *et al.* suggested [Ehre et al., 2010]. In addition, it cannot be ruled out that water vapor condensation may be influenced by pyroelectrically induced electric fields [Gao et al., 1999; Butt et al., 2011] and that the vapor condensation rate may be different between the opposite surface polarities due to very small droplets gaining a net positive charge after jumping from the hydrophobic surface [Miljkovic et al., 2013]. If the drop surfaces are charged, they can often favor coalescence as observed by the application of external electric fields [Ristenpart et al., 2009; Yokota and Okumura, 2011]. The mechanism of charge separation caused by the so-called contact electrification effect [Sun et al., 2016] might additionally influence the electric field-enhanced vapor condensation on the polar surfaces of a pyroelectric single crystal during the cooling process.

In light of the various experimental methods described above, it was de-

6

cided to use two measurement setups for the investigation of the correlation
between pyroelectricity and degree of supercooling. It was possible using
both setups to make conclusions about the reproducibility of the icing tem-
perature measurements: in one setup (sessile droplet method) the water is
deposited as a free-standing droplet and in the other setup water of the same
volume is enclosed in a ring system of a certain geometric size (ring sys-
tem method). The main difference is that the free-standing water droplet
is exposed to an air environment inside the heating and cooling chamber
as would be the case in natural surroundings (different from water in the
ring). In order to examine the effect of nitrogen gas on the control of the
air humidity around the droplets, icing temperature measurements with and
without nitrogen gas flow were compared against each other. In contrast, the
second setup with an enclosing ring system ensures a reproducible contact
area between the water and the crystal surface which is expected to improve
the comparability between different pyroelectric single crystal samples with
regard to the pyroelectrically induced ice nucleation.

2. Materials and methods

In the present paper, the degree of supercooling of water on different
pyroelectric single crystals was investigated. In order to determine the in-
fluence of the measurement setup on the icing temperature of supercooled
water, several water cooling experiments with and without a ring system,
and with and without nitrogen flow were performed.

Pyroelectric single crystals were used as the model systems because their
polarization vector can be aligned over the whole sample volume (polar axis

7

perpendicular to the parallel surfaces). In this paper the single crystal samples are labelled as follows: strontium barium niobate ($Sr_xBa_{1-x}Nb_2O_6$, FEE GmbH) as SBN, lithium niobate ($LiNbO_3$, CrysTec GmbH) as LN, and lithium tantalate ($LiTaO_3$, CrysTec GmbH) as LT. The dimensions of the single crystals and their pyroelectric coefficients p_{pyro} at room temperature are listed in Table 1.

Table 1: Physical and geometric properties of the different pyroelectric single crystals.

sample	material	p_{pyro} in $\mu C/(m^2 \cdot K)$	surface area in mm^2	thickness in mm
SBN	$Sr_xBa_{1-x}Nb_2O_6$	$300\ldots1100$ [a,b]	5 x 5 (*square*)	1.5
LN	$LiNbO_3$	$60\ldots83$ [a,c]	$\frac{\pi}{4}\cdot15^2$ (*circle*)	1.0
LT	$LiTaO_3$	$170\ldots230$ [a,d]	$\frac{\pi}{4}\cdot15^2$ (*circle*)	0.5

[a] [Joshi and Dawar, 1982; Newnham, 2005]

[b] [Glass, 1969]

[c] [Bartholomäus et al., 1994]

[d] [Putley, 1980; Ping and Lin, 1981]

Prior to the first experiment, all single crystals and rings were cleaned in an ultrasonic ethanol bath for a few minutes in order to remove external adsorbates, they were subsequently rinsed with deionized water and then air-dried for 30min. Between the experiments, all samples and rings were rinsed only with deionized water and then air-dried. The measurement setup for the ring system method, shown in the upper right part of Figure 1, consists of the ring system of a chosen material with inner and outer diameter of 3 mm and 5 mm, respectively, placed on the smooth (roughness $\leq$ 1 nm) pyroelectric single crystal sample. Aluminum rings were used in most experiments. A thin cover glass plate placed on the top of the ring prevented significant evaporation of the 10 μl deionized water that was dropped by a syringe into

8

the interior of the ring. In the sessile droplet method a number of water droplets of 10 μl volume were freely dropped on the single crystal sample (upper left part of Figure 1).
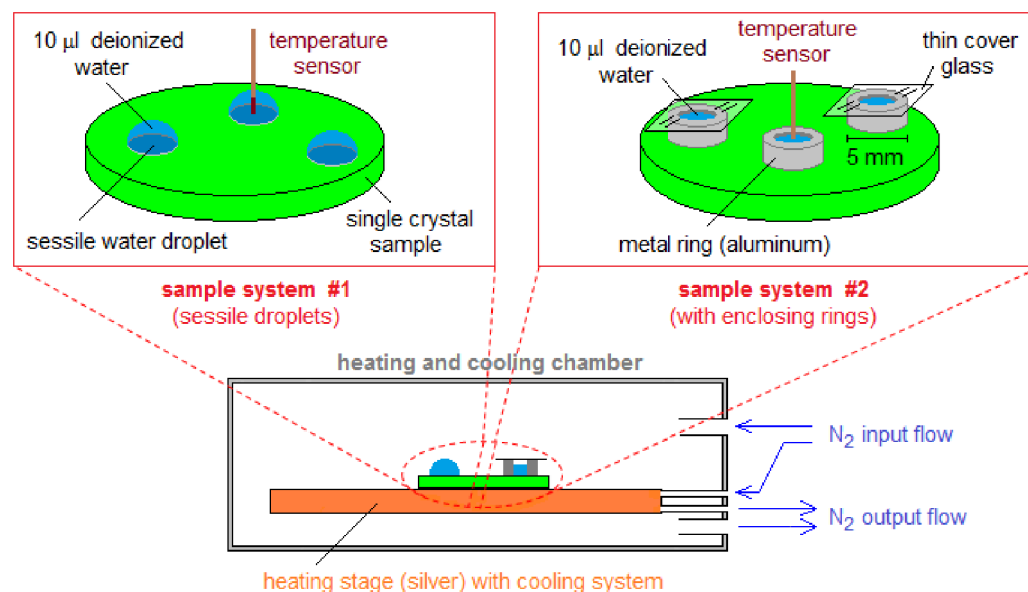

Figure 1: Sketch of the two used setups for the measurement involving a pyroelectric single crystal sample. In the sessile droplet method (upper left) free-standing water droplets were placed on the single crystal sample and in the ring system method (upper right) a thin cover glass prevents any significant evaporation of water from inside an aluminum ring. The sample system was put on a heating/cooling stage inside a Linkam chamber. An additional control system regulated the input and output flow of cold nitrogen gas during the cooling and heating process.

All icing measurements were made within a cooling chamber (Linkam LTS 350) containing a silver heating stage with integrated primary cooling circuit (internal nitrogen gas flow) and a thermocouple to control the temperature of the heating stage in the range of 25 ℃ and -25 ℃. For the sessile

9

droplet method, the chamber volume was in some experiments purged with a varying amount of cold nitrogen gas from a dewar connected to the Linkam LNP pumping system (external nitrogen gas flow). Before the start of a measurement cycle, the sample and drop/ring system was cooled down from room temperature to 5 ℃. This temperature was kept constant for 10 min, so that the entire volume of water inside the ring system was equilibrated to this temperature. Afterwards, the cooling rate was changed to 1 ℃/min and the whole sample system was cooled down to the final temperature of -25 ℃. All measurements involved temperature variation in order to activate the pyroelectric effect emerging from the single crystal samples. The magnitude of the change in polarization (ΔP) of the single crystal is determined by the pyroelectric effect p_{pyro} multiplied by the change in temperature ΔT. The creation of pyroelectrically induced net surface charge based on this effect therefore requires the controlled temperature variation of the heating/cooling stage. A circular window in the top of the chamber enables the visual observation of the water with the help of an optical microscope. During the cooling process the water experiences a phase transformation and, as a consequence, the optical transparency of the water changes from clear to white-opaque. At this point, the icing temperature was determined from the value indicated by the control system. After reaching -25 ℃, the sample and drop/ring system was heated back to 5 ℃ and held there for 10 min. Subsequently, a new measurement cycle was started.

In order to study the impact of the physical properties of the ring system on the icing temperatures measured on the pyroelectric single crystals, two other metal ring systems, one made of stainless steel and the second of

10

polyamide, were compared to the normally used aluminum ring system. The stainless steel ring was laser cut from a steel sheet with the same geometry as the aluminum ring and mechanically polished. The plastic ring system (polyamide) was mechanically cut and contained 7 holes which were equally separated in a plastic sheet of the same thickness/height as the metal ring system. The inner diameters of all the rings are identical in order to have geometrically equal measurement conditions with the same interfacial contact area between water and single crystal sample. The physical properties of the rings are presented in Table 2.

Table 2: The room temperature physical properties of the rings.

	aluminum	stainless steel	polyamide (PA, Nylon 6)
heat conductivity (W/m·K)	$\approx 236\ (210\ldots 240)$ [a,b]	$\approx 16\ (14\ldots 17)$ [a,b]	$\approx 0.25\ (0.16\ldots 0.33)$ [a]
specific heat capacity (kJ/kg·K)	$\approx 900\ (880\ldots 921)$ [a,b]	$\approx 500\ (450\ldots 530)$ [a,b]	$1670\ (1500\ldots 2800)$ [a]
thermal diffusivity (mm^2/s)	≈ 97 [(*)]	≈ 4 [(*)]	≈ 0.16 [(*)]
surface roughness (μm)	$0.2\ldots 1.5$ [(**)]	$0.2\ldots 1$ [(**)]	$1\ldots 20$ [(**)]

[a] MatWeb (the searchable database of material properties, www.matweb.com)

[b] *Tables of Physical and Chemical constants* (16th edition, 1995), Kaye & Laby Online, www.kayelaby.npl.co.uk

[(*)] calculated with values from [a]

[(**)] estimated from SEM measurements (see supplementary material).

During the cooling process, the temperature of the cooling stage on which the pyroelectric crystal was placed was always lower than the water temperature, because of the time-dependent temperature profile of the water during the cooling process. The temperature profile does not only depend on the

11

sample thickness, but the thermal conductivity of the sample and stage material, as well as the environment around the water. Therefore, a temperature sensor (K-type thermocouple Microchip MCP9804) was put into a secondary water drop on the pyroelectric surface and the water temperature was measured together with the stage temperature. Temperature measurements were made in order to provide information on the actual water temperature near the solid-liquid interface, which is unfortunately not taken into account in many icing studies. From these temperature measurements calibration curves were obtained in order to equate the water temperature at the solid-liquid interface with the cooling stage temperature. This approach is advantageous since a temperature sensor is not needed in all further icing temperature measurements, thereby simplifying the experiment. However, such an approach is only valid if a separate calibration curve is set up for each sample-system combination (with or without ring system, geometry and type of the sample, water volume).

At least 20 measurement values were obtained for each sample in both measurement setups in order to evaluate the icing temperature distribution. By using the Weibull cumulative distribution function to capture the probability of a freezing event [Weibull, 1951; Johnson et al., 1994], the mean icing temperature could be determined at the 50% probability within a 10% - 90% confidence interval [Wilson et al., 2003; Wilson and Haymet, 2012]. The length of error bars were calculated to be two times the standard deviation (2σ) of these measurement values. The uncertainty of the temperature measurement itself is determined by the systematic error of the temperature control system and has a maximum value of 0.2 ℃.

12

3. Results

3.1. Calibration curves of water temperature at the solid-liquid interface

The measurement procedure described in section 2 was used to obtain water temperatures T_w in the liquid phase for every 2 ℃ of the heating stage temperature T_{hs} starting from 4 ℃ down to the freezing point. After collecting water temperature values from at least two cooling runs, the measured data were plotted and fitted for all three pyroelectric single crystal samples as shown in Figure 2 for the cases of a free-standing water droplet and water in the aluminum ring system.
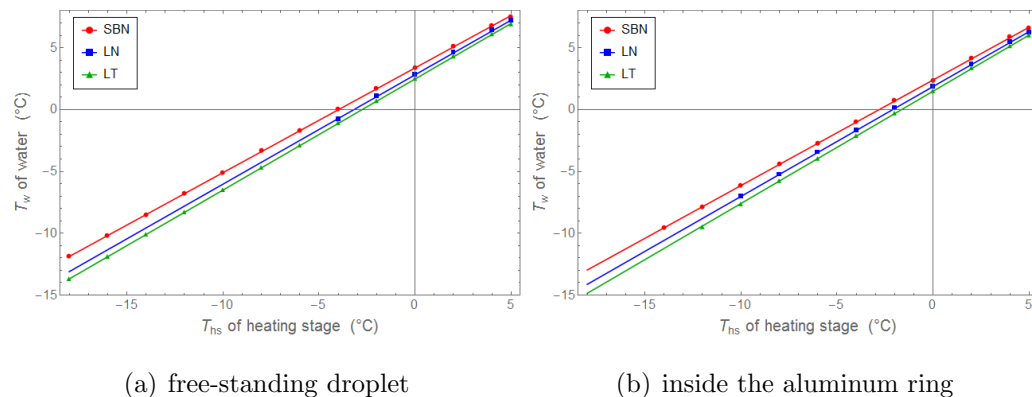

(a) free-standing droplet   (b) inside the aluminum ring

Figure 2: Calibration curves of water temperature T_w of (a) free-standing droplets and (b) inside the aluminum ring on three different pyroelectric single crystal samples (named in the legends) as a function of the heating stage temperature T_{hs}.

In both Figures 2 (a) and (b) linear curve fits were applied for each pyroelectric single crystal (fit parameters shown in Table 3). They were found to be nearly collinear, however, their slopes depend on the sample thickness and thermal conductivity, which means that a flatter fit curve is due to retarded heat transfer from the silver cooling stage through the sample

13

Table 3: Fit functions of water temperature on all three pyroelectric single crystal samples for both measurement setups.

sample	free-standing droplet	inside the aluminum ring
SBN	$T_{w,\mathrm{SBN}} = 0.847 \cdot T_{hs} + 3.380$	$T_{w,\mathrm{SBN}} = 0.854 \cdot T_{hs} + 2.402$
LN	$T_{w,\mathrm{LN}} = 0.885 \cdot T_{hs} + 2.821$	$T_{w,\mathrm{LN}} = 0.889 \cdot T_{hs} + 1.873$
LT	$T_{w,\mathrm{LT}} = 0.898 \cdot T_{hs} + 2.483$	$T_{w,\mathrm{LT}} = 0.908 \cdot T_{hs} + 1.496$

to water at the surface of pyroelectric single crystal. In addition, the slightly different initial temperature values at a stage temperature of 5 ℃ after 10 minutes are due to the different equilibrium temperatures caused by the difference in thermal conduction of the samples. By comparing the fit curves of both cases (Figure 2 (a) and (b)) it can be seen, that the temperature of water in the aluminum ring during the cooling process is about 1 ℃ lower than that of the free-standing water droplets for each substrate (at -16 ℃ stage temperature). This temperature difference can be explained by the inhibited heat transfer from the slightly warmer air to the water volume inside the ring (as if the ring produces an extended cooling surface area). The fit function of the water temperature inside the plastic ring system on LN is given by $T_{w,\mathrm{LN}} = 0.883 \cdot T_{hs} + 1.733$ for comparison. For temperature below 0 ℃ the water temperature inside the aluminum ring system differs less than 0.1 ℃ from that inside the plastic ring.

3.2. Icing temperature of "free-standing" water droplets (sessile droplet method)

3.2.1. Without additional nitrogen gas flow

For these experiments, water droplets of the same volume (10 µl) were placed on each pyroelectric single crystal sample and were exposed to the ambient air in the chamber. This measurement setup provides an insight

14

into the influence of contact area of the water droplet with the pyroelectric single crystal and the effect of heat transfer through the air/water interface.
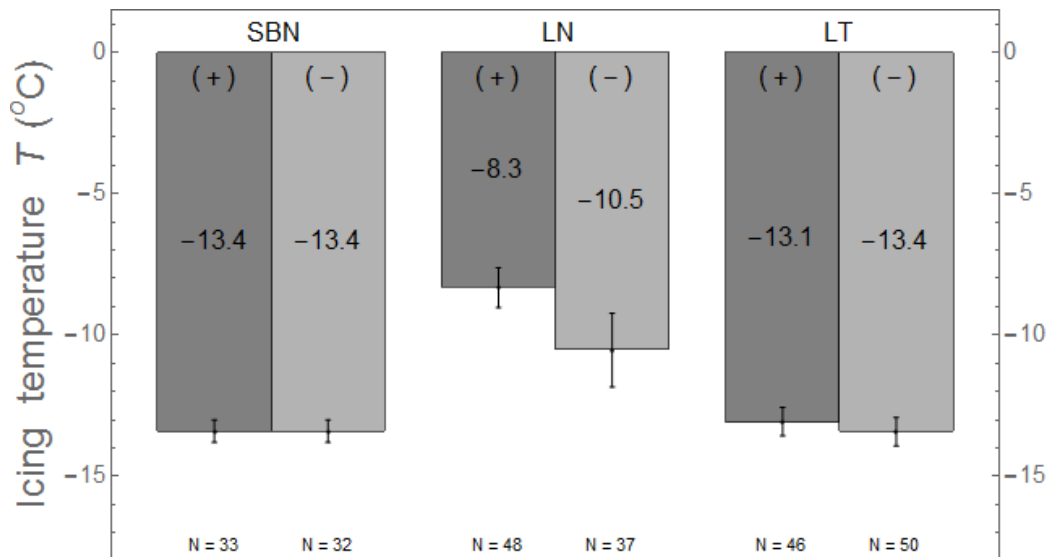

Figure 3: Icing temperatures of a free-standing water droplet on the oppositely charged surfaces of the three different pyroelectric single crystals. The darker bars indicate the positively charged surfaces and brighter bars the negatively charged surfaces. The inset "N =" at the bottom of the figure indicates the number of measurements made for the corresponding bar.

The bar chart in Figure 3 shows the icing temperatures on the oppositely charged surfaces of the three different pyroelectric single crystals when undergoing a cooling with a constant rate of 1 ℃/min. The water droplets on these single crystals display supercooling of more than 8 ℃ relative to the ordinary freezing point of 0 ℃ (at ambient pressure of 1 atm). Out of all tested pyroelectric single crystals, both surfaces of the LN sample showed the highest icing temperatures. Of the three pyroelectric single crystals, LN

15

possesses the lowest pyroelectric coefficient, see Table 1. This suggests that there could be a correlation between the pyroelectric coefficient and the icing temperature. However, a clear dependence of the amount of supercooling on the pyroelectric coefficient is not supported by the comparison between the SBN and LT samples, which reveal nearly the same icing temperatures, although the pyroelectric coefficient of SBN is considerably higher than that of LT (see Figure 3 and Table 1). A longer discourse about the connection between icing temperature and pyroelectric coefficient will be outlined in the discussion section. The negatively charged surface of LN has a 2 ℃ lower icing temperature compared to the positively charged surface, whereas the differences on both oppositely charged surfaces of SBN and LT are within the error bars (see Figure 3).

3.2.2. With additional nitrogen gas flow

The icing measurement of free-standing water droplets was repeated under nitrogen gas flow conditions. A comparison between the two conditions for the SBN and LN samples are shown in Figure 4.

The SBN sample shows slightly higher icing temperature when exposed to a nitrogen gas flow compared to when there is no flow. While the icing temperatures of water on negatively charged surfaces of LN show no significant differences between the two conditions, the variation of freezing temperatures on positively charged surfaces is higher (see Figure 4).

3.3. Icing temperature of water inside an aluminum ring (ring system method)

For these experiments, the same volume of water was enclosed by an aluminum ring on a pyroelectric single crystal sample. This measurement
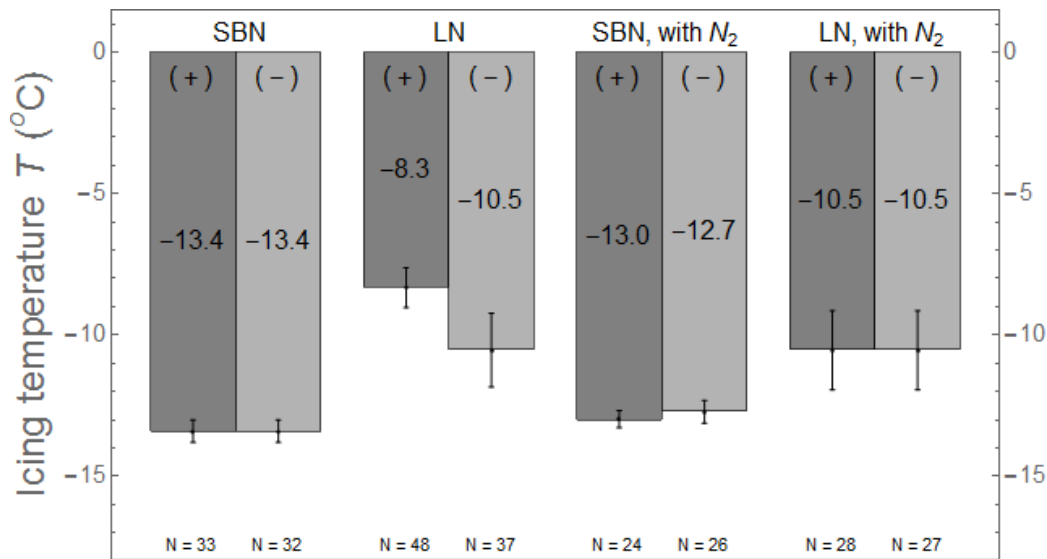
16

Figure 4: Icing temperature of a free-standing water droplet on the oppositely charged surfaces of two different pyroelectric single crystals without (left bar group: SBN and LN) and with nitrogen gas flow (right bar group: SBN, with N_2 and LN, with N_2).

setup, different from the sessile droplet method, provides a constant fixed contact area of water with the pyroelectric sample and a better isolation of the system from the surrounding atmosphere.

This setup leads to different icing temperatures (see Figure 5 in comparison to Figure 3). The icing temperatures are lower (sometimes significantly) for the water in the ring placed on the various sample surfaces compared to the sessile water droplets on the same surface. The possible reasons for this dependence of the freezing behavior will be outlined in the discussion section. In Figure 5 it can be seen for SBN and LT that the negatively charged surface of the pyroelectric single crystal tends to lower icing temperature than the positively charged surface. The difference in the freezing temperatures of the

17

enclosed water on positively and negatively charged LN surfaces lies within the error bars.
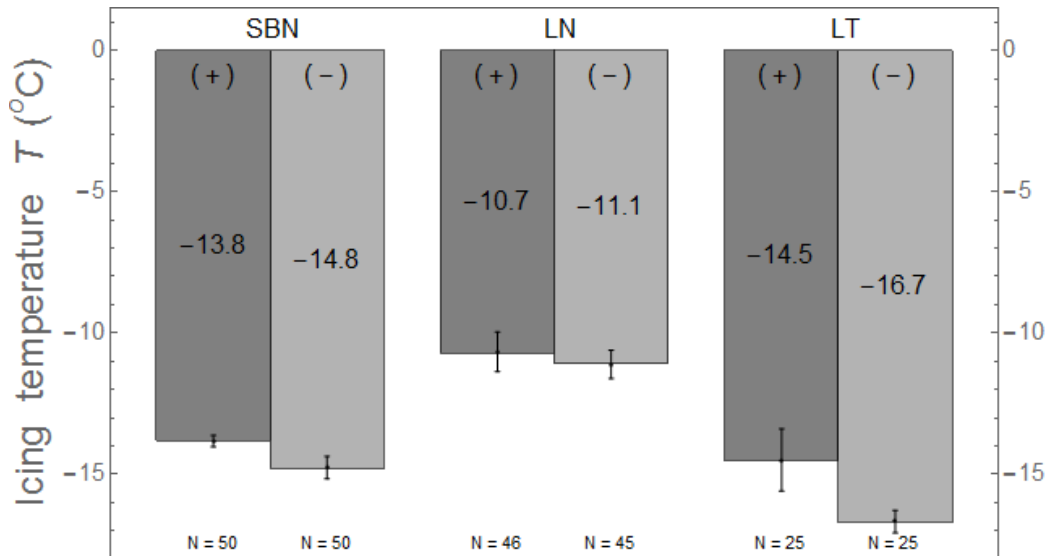

Figure 5: Icing temperatures of water inside an aluminum ring lying on the oppositely charged surfaces of the three different pyroelectric single crystals.

3.4. Comparison between icing temperatures of water in ring systems of three different materials

For this experiment only the LT single crystal sample was chosen because out of all the three pyroelectric single crystals it showed the lowest icing temperature and the largest temperature difference between the oppositely charged surface sites (see Figure 5). Although all ring systems had the same geometrical size (same hole diameter and ring height), the icing temperature of water strongly varied between the various materials. Water in the aluminum ring achieved the lowest icing temperature on both the surfaces

18

of LT and was 5 to 7 ℃ lower than when a steel ring was used (see Figure 6). The icing temperatures of water inside the plastic ring lay between those of the aluminum and steel ring, despite its heat diffusivity being much lower than that of both metals. This finding indicates that other factors in addition to the heat conduction have an influence on the degree of supercooling that can be achieved. Two possible differences are the interfacial influence on the heat transfer (heat transfer coefficient and emissivity of the ring material) and the surface roughness. Although the inner wall of the ring system was polished, a surface roughness of up to a few micrometers might be present, which would be expected to act as potential active sites for heterogeneous ice nucleation. Of the three ring systems, the aluminum ring appeared to have the smoothest inner wall surface (see supplementary material for further information about the surface roughness), which is suggested to lead to the lowest icing temperatures.

4. Discussion

4.1. Relationship between pyroelectricity and the degree of supercooling

The results of the icing temperature measurements suggest that the degree of supercooling of water droplets varies between the different pyroelectric single crystals. The LN single crystal, which has the lowest pyroelectric coefficient of all the three tested samples, exhibited the highest icing temperature. Contrastingly, the two other pyroelectric single crystals (SBN and LT) with significantly higher pyroelectric coefficients caused lower icing temperatures. On these surfaces the water freezing process was more impeded compared to the process on the LN single crystal, by at least 2.5 ℃ (see Figure 3 and 5).
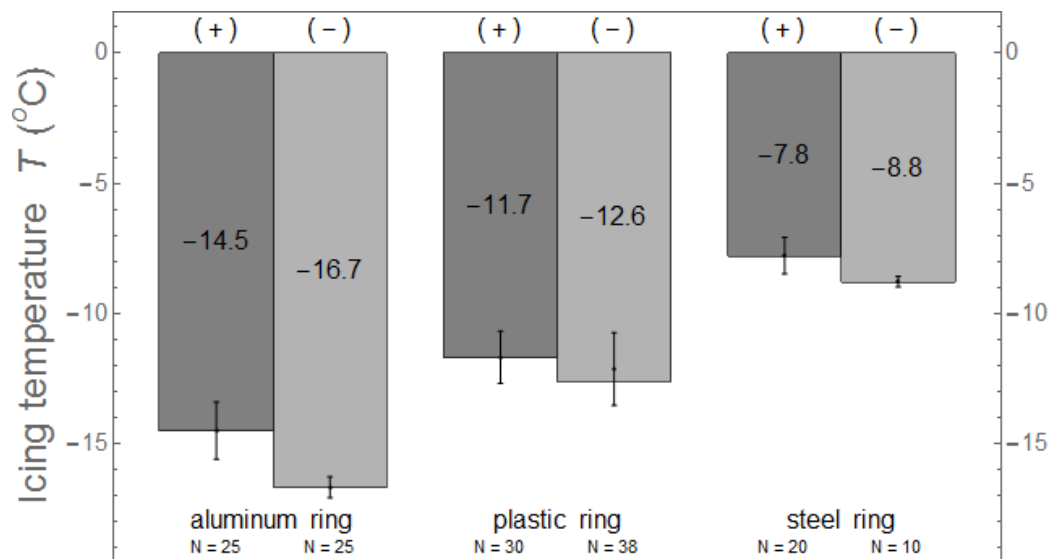
19

Figure 6: Icing temperatures of water in the three ring systems of different materials lying on oppositely charged surfaces of the pyroelectric LT single crystal.

Based on this finding, it can be assumed that the icing temperature of water decreases when the pyroelectric coefficient of a single crystal sample is larger. However, the applicability of this view is challenged by the similar icing temperatures measured on the SBN and LT single crystals (see Figure 3 and 5), despite the SBN single crystal having the highest pyroelectric coefficient (see Table 1). It seems, and has been suggested by Damjanovic *et al.* and Lang *et al.*, that there might be an upper threshold of the coefficient above which any increase of surface charge induced by the pyroelectricity does not produce a further ice-delaying effect [Damjanovic, 1998; Lang, 2005]. The pyroelectrically induced surface charge is expected to form an electric field at the surface that decays into the body of the water due to electrostatic screening caused by the presence of mobile charge carriers in water and its

20

permittivity [Butt et al., 2003]. Consequently, it can be assumed that the electrochemical interface processes in the presence of the surface charge induced electric field are additional factor affecting the formation of hydrogen bonding networks prior to the heterogeneous ice nucleation.

In all of the measurements in which there was a significant freezing temperature difference the negatively charged surface of the pyroelectric single crystal caused a lower freezing temperature compared to the positively charged surface. Therefore, the heterogeneous ice nucleation was more strongly impeded on the negative surface. This may be explained either by the polarization dependent ordering of water molecules near the solid surface or the surface structure, which prefers specific bonding configurations that in the case of the negative polarized surface would be expected to lead to the inhibition of ice crystallization.

The experimental methods used in this work cannot provide a deep insight into the interfacial processes described above, as a consequence, the focus was laid on the impact of the experimental method on the water freezing. The results obtained in this work for each of the single crystals have much smaller icing temperature differences between the oppositely charged surfaces than those measured by Ehre *et al.* [Ehre et al., 2010]. Some differences are within the error bars and these results do not fully support the anti-icing properties of negatively polarized pyroelectric surfaces. Additionally, there are several factors which may superimpose or dominate the pyroelectric contribution to the heterogeneous ice nucleation and they are discussed in the next sections.

21

4.2. Influence of measurement systems and external factors on icing temperature

4.2.1. Free-standing droplet and influence of nitrogen gas flow

The environmental conditions surrounding the free-standing water are different from those experienced by the water inside the ring system due to the presence of an air-liquid interface across the whole hemisphere of the water droplet. As a consequence, the extension of the air-liquid interface can determine the stochastic nature of the heterogeneous ice nucleation, as the extended area is different from the solid-liquid interface on the inner wall of the ring system. Free-standing water droplets that are fully exposed to the air environment inside the chamber undergo gas-liquid vapor exchange due to the inter-diffusion of water vapor and gaseous molecules near the air-liquid interface. The dissolubility effect of gas molecules by diffusion from the air is an entropic effect and increases with decreasing temperature [Frank and Evans, 1945; Guillot and Guissani, 1993; Rettich et al., 2000; Koga, 2011; Abe et al., 2014; Cerdeirina and Debenedetti, 2016]. Dissolved gases in water can alter the molecular structure of water due to reactions of solutes with the solvent [Scheraga, 1965; Ashbaugh and Paulaitis, 2001; Oleinikova and Brovchenko, 2012] and the associated physicochemical processes [Workman and Reynolds, 1950; Bronshteyn and Chernov, 1991; Takenaka and Bandow, 2007], [different types of mechanisms are described in O'Concubhair and Sodeau, 2013]. The associated alteration of the hydrogen bonding network can lead to a variation in the freezing rate compared to that of pure liquid water [Parungo and Lodge, 1967; Kashchiev and Firoozabadi, 2002; Kletetschka and Hruba, 2015]. It has also been shown that the convective heat conduc-

22

tion in water was hindered by the gases dissolved in the water, leading to an increase in the enthalpy of the water freezing process [Wojciechowski et al., 1988]. A variation of gas content in water also changes the heat flow homogeneity during the cooling process. The heat flow through water with a low gas content is more uniform than that for the case where there is a higher gas content and, in addition, it is attenuated in the vicinity of the gas-liquid complexes. Due to the poor heat conduction properties of gases incorporated in these complexes, water containing more dissolved gases has a lower effective cooling rate and, therefore, it is expected to have a stronger influence on freezing compared with water with less gas content. Several studies have reported on an enhancement in ice crystallization occurring at the air-liquid interface relative to the main body of the water. This has been suggested to be due to crystal nucleation at the droplet surface being thermodynamically favored over nucleation within the main volume [Djikaev et al., 2002; Tabazadeh et al., 2002; Shaw et al., 2005]. By comparing the freezing temperatures measured with either the aluminum ring or for the sessile droplets, no change can be seen for SBN, the change for LN is within the error bars but a significant change occurs for LT. For the LT, the freezing delay was significantly larger when the water was inside the ring system and therefore more isolated from the surrounding atmosphere. For all droplets water from the same prepared batch was used, the effect might therefore be more dominated by the specific interaction of LT with the solved gas than by the interactions between the gas molecules and the liquid-gas interface in general.

The usage of nitrogen gas instead of air in a closed chamber as described

23

in 3.2.2 avoids possible water surface chemistry caused by such gases as O_2 and CO_2. The solubility of nitrogen in water is about twice that of oxygen in water (O:N=1:1.8) [Murray and Riley, 1969; Weiss, 1970], consequently, the ratio of O:N in the water is changed in comparison to air (1:4). The experimental work on the influence of nitrogen gas flow on icing temperature presented in this study (Figure 4) does not unambiguously determine any amount of altered freezing behavior: on negatively charged surfaces the icing temperature does not change significantly (0.5 ℃ maximum), whereas relatively larger temperature changes of at least 1 ℃ were measured on positively charged surfaces. The magnitudes of the temperature change between oppositely charged surfaces for the cases of air and nitrogen flow environments are insignificant i.e. less than the measurement uncertainty. The main purpose for the introduction of nitrogen gas into the Linkam chamber in these experiments was to reduce the air humidity near the sample/water droplet. It is expected that the nitrogen gas streaming around the water droplets mitigates vapor condensation onto the cold sample surface by carrying off any water vapor from the vicinity of droplets. As a consequence, it can be anticipated that the influence of condensation-induced frost formation is reduced. In high humidity environments the formation of condensed droplets starts on the cold sample surface adjacent to the water droplets and could be expercted to trigger water droplet freezing via the growth of ice bridges propagating across the surface [Guadarrama-Cetina et al., 2013; Boreyko et al., 2016]. Jung *et al.* showed experimentally the effect of environmental humidity and gas flow on the ice crystallization mechanism on supercooled surfaces [Jung et al., 2012]. In the experiments presented in this work, a significant

24

reduction of the air humidity due to nitrogen streaming inside the Linkam chamber is not confirmed as condensed microdroplets could still be seen on the silver heating stage. This indicates that the nitrogen flow rate or velocity inside the Linkam chamber was not sufficiently large enough to carry off a large number of water vapor molecules out of the chamber. Nevertheless, a faster decrease of the sessile droplet volume was observed after a few measurement cycles when there was the additional nitrogen gas flow compared to when there was no flow. After 3 measurement cycles the contact angle and the volume of the sessile water droplets exposed to nitrogen gas flow were about 15-25% lower than at the start of the experiment. For comparison, the contact angle and volume of the droplet without nitrogen flow decreased by no more than 15% compared to the initial values. Consequently, it is possible to conclude that the effect of the evaporation rate change due to the nitrogen gas streaming has a more pronounced effect than the associated reduction in air humidity on the icing temperature of sessile water droplets. This finding might explain why there is no further lowering of the icing temperature with nitrogen flow below the lowest value obtained in the absence of nitrogen gas flow, see Figure 4.

In many experiments of sessile droplet, a fast change of the water optical transparency happened before the ice front slowly moved from the bottom to the top of the frozen droplet, until the top of the droplet takes an icy cusp shape. In most cases this cusp-like shape on the top of already frozen water droplets was observed. The presence of the ice cusp on the top droplet surface indicates that the water solidification has started from the bottom of the droplet (water-sample interface) and the freezing front has moved upwards

25

to the top of the droplet. This upwards movement of the freezing front confirms that the water freezing was mainly triggered by the heterogeneous ice nucleation at the interface between water and the sample surface [Wang et al., 2006; Enrquez et al., 2012; Snoeijer and Brunet, 2012; Singh and Singh, 2013; Marín et al., 2014; Schetnikov et al., 2015]. This assumption is valid for the experiments in this work because the solid-liquid interface is the coldest point of the sessile droplet compared to the interface in contact with the warmer air during the continued cooling of the silver stage. For the case of no or weak nitrogen gas flow, the energy barrier for the heterogeneous ice nucleation at the solid-liquid interface is still energetically more favorable compared to the quasi-homogeneous nucleation at the air-liquid interface of the sessile droplet. An estimation made of the droplet volume change due to evaporation indicates only a small evaporation rate coefficient change can be attributed to the case of weak nitrogen gas flow compared to no flow. The low flow velocity of nitrogen gas around the sessile water droplet is at least one order of magnitude lower than that measured by Jung *et al.* [Jung et al., 2012]. Their measured flow velocity of 3 m/s leads to a remarkable reduction ($\Delta T = 0.34$ K at $T = $ -15 ℃) of water temperature at the air-liquid interface which moves the icing probability in favor of homogeneous nucleation compared to heterogeneous nucleation. Their observation of the first (recalescent) stage of the droplet freezing confirms the air-liquid interface as the onset point of freezing of the sessile droplet under shear flow [Jung et al., 2012]. The relatively lower flow velocity in the experiments presented in this work is not sufficient to cause a significant local temperature reduction at the air-liquid interface of the sessile droplet and, subsequently, effectively

26

reduce the energy barrier of the quasi-homogeneous nucleation. For both conditions tested, where the solid-liquid interface is the coldest point and there is weak nitrogen gas flow, the water freezing process is in all probability going to start at the water-substrate interface. This was also suggested by Jung *et al.* to be the case when there was no nitrogen gas flow [Jung et al., 2012].

4.2.2. Influence of the ring system and surface roughness on water freezing

Water in the aluminum ring achieved the lowest icing temperature on both the surfaces of LT and was 5 to 7 ℃ lower than when a steel ring was used Figure 6. The aluminum ring system leads to icing temperatures lower than those measured for the free-standing water droplets. The measurement of icing temperature of water enclosed inside a ring system is suggested to have advantages with regard to the setup reproducibility between different single crystal samples. The same contact area between the water and pyro-electric single crystal sample as well as a more homogeneous heat transfer through the symmetrical ring system ensure more controlled experimental conditions. The thin glass sheet covering the ring system prevents significant evaporation of water during the measurement, which helps to keep the water volume constant. The limited amount of gas molecules confined between the ring system and the cover glass restricts significant further penetration of oxygen from the air into the water, which could cause a change of water activity due to solvation of oxygen molecules or alternation of water structure [Heidt and Ekstrom, 1957; Heidt and Johnson, 1957; Hayon, 1962; Curtiss and Melendres, 1984; Knopf and Alpert, 2013]. The usage of the aluminum ring in these experiments is the best choice due to the acquisition of simi-

27

lar or lower measured icing temperatures compared to those measured with the sessile droplet method (Figure 3 and 5 for comparison). This implies that any contributions related to the inner wall of the aluminum ring do not initiate water freezing above the icing temperature measured for sessile water droplets lying on the same single crystal sample. For comparison, the mean icing temperature of free sessile water droplet placed on a polished aluminum sheet is measured to be -12.9 ℃ with a 2σ standard deviation of 2.4 ℃. The noticeable icing temperature differences between the ring systems can be possibly explained by differences in surface roughness influencing the ice nucleation process (see supplementary material). The importance of such a possibility is highlighted by the significant temperature difference between the two metal ring systems (aluminum and steel in Figure 6), which cannot be explained by the different thermal diffusivities alone (see Table 2).

Besides the pyroelectric contribution, the surface roughness and lattice parameters of the different single crystals could be expected to affect the heterogeneous ice nucleation. In general, nano- or microscale surface roughness has been shown to affect the wetting properties of the surface and to prevent or initiate heterogeneous ice nucleation depending on the exact environmental conditions (their effects on nucleation behavior are summarized in [Schutzius et al., 2015; Kreder et al., 2016]). Since all used single crystal samples have very smooth surfaces of roughness less or equal to 1 nm, this contribution on the comparison of the icing temperature between different samples can be excluded.

The icing temperatures of water on LN and LT differ widely (Figure 3 and 5), although both samples have the same crystallographic crystal structure

and similar lattice parameter (supplementary material). Therefore neither the surface roughness nor the lattice mismatch between the pyroelectric single crystal and ice crystals are expected to be the dominant factors that could possibly overshadow the pyroelectric contribution.

4.3. Other factors affecting water freezing

4.3.1. Electric field from the sample

During cooling a concurrent change of the spontaneous polarization inside the pyroelectric crystal results in a variation of the surface charge on both polar surfaces. This surface charge modifies the wetting properties of the crystal surface when measuring with the sessile droplet method. It causes the droplet to spread while lowering the contact angle and increasing the contact area. This phenomenon of electrowetting can be understood in terms of the electrostatic forces acting on the droplet, where the strength of its impact depends on the pyroelectrically induced surface activity of the crystal. As a consequence, the contact angle and thus the contact area of the droplet on different crystal surfaces are expected to vary due to their different pyroelectric properties. Although the Young-Lippmann electrowetting equation describes a decrease of the contact angle with increasing applied electric field regardless of its polarity, a few studies have shown polarity effects on electrowetting, which was linked to molecular processes at the solid-liquid interface ([see the section 3.2.2 of Chen and Bonaccurso, 2014], [Moon et al., 2002; Fan et al., 2007; Koo and Kim, 2013]). In the experiments presented in this work, sudden changes of the droplet shape from a circular to oval contact area were observed on both surfaces of LN. The alternation of the air-water surface area and the contact area caused by the electrowetting-

29

induced change of the droplet shape can be expected to exert an impact on the heterogeneous nucleation rate during water supercooling.

4.3.2. Influence of contact area on icing temperature

The sessile water droplets were found to form an almost hemispherical shape after being dropped on the flat surface of a pyroelectric single crystal sample. The sessile droplet surface takes on a certain static contact angle with respect to the flat surface, where its magnitude depends primarily on the surface tension at the solid-liquid interface. As a consequence, water droplets deposited on surfaces of different single crystal materials are be expected to exhibit different contact angles, if these materials have differing surface energies (interfacial energies, see supplement material for further information). For a constant water droplet volume the contact area between the water droplet and solid surface is a function of the contact angle. The ratio between the free droplet surface area (spherical cap - A_{cap}) and the contact area (base of the spherical cap - A_{base}) varies with the contact angle as:

$$C(\theta) = \frac{A_{\mathrm{cap}}}{A_{\mathrm{base}}} = \frac{2\pi r^2 (1 - \cos\theta)}{\pi r^2 \sin^2\theta} = \frac{2}{1 + \cos\theta}$$

where r is the radius of the virtual sphere and θ is the contact angle. This spherical cap model is only valid for small droplet volumes less than 20 μl, where the gravitational effect on the droplet shape is negligibly small. The contribution of the gravitational potential energy on the equilibrium droplet shape of a 10 μl drop is about 5% of the interfacial energy (Young equation) for the contact angle range between 60 and 120 ° (calculated using the energy equations in [Shapiro et al., 2003] - compared to 7% - 9% for 20

30

μl). In the experiments presented in the supplementary work the contact angle lay within the angle range of 60 and 85 ° and the corresponding ratio $C(\theta)$ was in the range of 1.3 and 1.9 (Figure 7). This indicates that there is a non-vanishing interfacial effect on water freezing since the icing temperature depends on the contact angle and thus the contact area (droplet diameter) of the water droplet [Langham and Mason, 1958; Alizadeh et al., 2012; Huang et al., 2012; Ishikawa et al., 2014; Zhang et al., 2016]. For comparison, the ratio of the liquid-ring surface area to the contact area for the case of the ring system method amounts to 1.886 for a 10 μl water volume. This lies in the upper range of the ratio $C(\theta)$ for the case of the free sessile water droplets.

4.4. Concluding remark of the discussions

An unambiguous influence of the pyroelectric effect on the freezing delay could not be extracted from these experiments due to the influencing factors described in detail above. This assertion is supported by the relatively small icing temperature differences of droplets on the oppositely charged surfaces compared to the results of the experimental study led by Ehre *et al.* [Ehre et al., 2010]. It has been suggested that the pyroelectrically induced freezing effect is overshadowed by the interplay of all the additional influence factors and their interaction with the specific single crystal surfaces.

A summary of the advantages and disadvantages of the two measurement setups with regard to their influence on the water freezing process is given in Table 4.

It is evident from the sections 4.1 to 4.3, that the icing temperature strongly depends on the experimental setup and their related influence factors. As a consequence, it is appropriate to link the outcome of the measure-
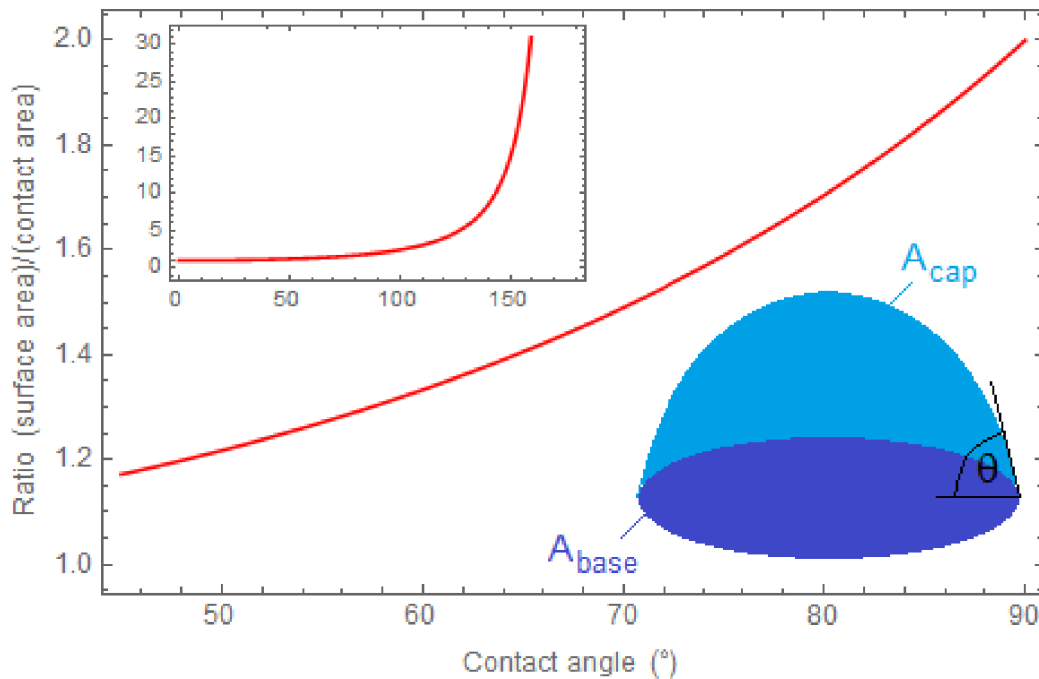
31

Figure 7: The ratio between the free surface area A_{cap} and contact area A_{base} of the sessile water droplet (shown in the lower right) as a function of the contact angle θ. The inset shows the ratio in the full range of contact angle from complete wetting ($\theta = 0\,°$) to complete dewetting ($\theta = 180\,°$).

ment to the chosen experimental setup. In order to make a decision about which experimental method is the best, it is necessary to be aware of the advantages and disadvantages listed in Table 4 depending on to what purpose the obtained results will be applied (e.g. liquid container or water droplet in natural environment).

In order to investigate the contribution of the pyroelectric effect on the water freezing process without any consideration needing to be paid to other factors affecting the freezing, i.e. ensuring the same experimental conditions, then a ring system is the most suitable method. Otherwise, when the results

32

Table 4: Advantages and disadvantages of the used measurement setups.

free sessile water droplet	water in the ring system
advantages:	*advantages*:
+ better comparison of icing temperature values to those measured in nature due to the more comparable environmental conditions (water freezing controlled by the contact angle of the droplet determined by the material properties of the sample)	+ better comparability between different samples due to the same geometric size (equal contact area between water and sample surface)
+ a lower number of interfaces (water-air, water-substrate)	+ constant water volume due to negligible evaporation in the limited space inside the ring system closed by the cover glass plate
	+ lower temperature gradient between the crystal surface and free surface of water due to the good heat conductivity of the metal ring system
disadvantages:	*disadvantages*:
− effect of evaporation and connected decrease of water droplet volume on water freezing temperature	− inner wall influence due to heterogeneous effect on water freezing (surface roughness, thermal properties)
− relatively strong variation of contact angle and contact area of the droplet over time	− confinement situation of water leads to different freezing behavior than would be expected in nature
− influence of air humidity due to vapor condensation and related formation of ice bridges on cold sample surface	

should be used for the case of water freely exposed in a natural environment, the sessile droplet method yields the most relevant results. Although a lot of experimental studies about water freezing have been conducted by others, the results of these findings cannot be collated due to the large range of diverse experimental methods used, i.e. the reproducibility gets lost in the

methodological diversity. As a consequence it has been a goal of this work to highlight this problem and to stress the necessity for common methodological standards of experimentally determined icing/freezing temperatures to be compared in a meaningful way.

4.5. Additional remarks and suggestions for improvements

4.5.1. Influence of spatial distance between droplets

Before performing measurements on sessile water droplets, care had to be taken while dropping the water droplets in order to ensure the spatial distance between the adjacent droplets was at least three times the droplet diameter. This approach was found to prevent the undesirable simultaneous water freezing of multiple droplets caused by the formation of vapor condensation-induced ice bridges between the droplets.

4.5.2. Chamber size determines the spatial temperature distribution (temperature gradients)

For these experiments a Linkam LTS 350 heating and cooling chamber was used due to its compact size, easy-to-use setup and low usage of nitrogen gas for the coolant. This setup provides a bottom-up cooling from the stage (silver plate) through the sample to the water and air. In this chamber it is expected that because of the small distance between the silver heating stage and the metal chamber cover, in combination with poor thermal isolation around the chamber, relatively large temperature gradients exist within the chamber during the cooling process. In some additional measurements a temperature sensor was placed at different positions inside the chamber (in contact with the silver stage and a few mm above the silver stage) and the

34

local temperatures were measured. The results showed a surprisingly large difference in their time-dependent behavior as the stage was cooled. The air temperature at a distance of a few mm above the silver stage was always measured to be above 0 ℃, while the temperature of the silver stage during the cooling process was far below this value, i.e. the measured temperature difference between the positions (with a separation of a few mm) exceeded 10 ℃ in most cases. Such large temperature gradients of at least 5 ℃ along the normal to the sample-stage are expected to exert a strong unwanted influence on the freezing behavior of the water droplet. The presence of this gradient would suggest that this is a non-realistic freezing situation compared to the typical situation encountered by freezing droplets in nature, where much lower temperature gradients exist in the volume around the sessile droplet (the air temperature can be below 0 ℃). Therefore, it would be desirable to use a larger chamber with appropriate thermal isolation that can ensure more uniform temperature distribution and lower temperature gradients inside the chamber.

5. Conclusion

The presented measurements suggest that the ascertainable freezing temperature reduction of water droplets on different pyroelectric single crystal samples and the degree of supercooling was found to vary between different pyroelectric single crystals. In a few cases the negatively charged surface of a pyroelectric single crystal promoted additional supercooling of the water before freezing took place in comparison to the positively charged surface, although the icing temperature difference was often not as large as measured

35

by others. A possible correlation between the pyroelectric coefficient and icing temperature was found only within a certain range of the coefficient.

The presented experimental studies have demonstrated that different experimental methods lead to measurable differences in the icing temperature due to the influence of various external factors. Most notably the material type of the ring system has a significant influence on the experimental outcome. In contrast to the water in the ring system method, a sessile droplet is more exposed to the air environment and, as a consequence, it is subjected to several external factors, e.g. air humidity, nitrogen gas flow in the chamber etc. Moreover, contact angle and related contact area variation due to droplet evaporation influence the freezing behavior. An additional influence comes from possible frost formation on the sample surface. These spurious affects have caused higher icing temperatures in our experiments than measured for the water enclosed in the aluminum ring system.

On the basis of these findings for two measurement methods, it is clear that there is a strong connection between the obtained result and the used measurement setup. Moreover, this problem is expected to apply to the large variety of methods used in the literature. It is, therefore, essential to make a methodological analysis of the water supercooling and freezing process. Further investigations are needed in order to analyze the many other factors affecting water freezing, e.g. air humidity, temperature distribution inside the chamber, and heat transfer through the water droplet, in addition to the pyroelectric effect.

36

Acknowledgement

Appendix. Supplementary material

The supplementary material is available free of charge on the Elsevier's website at DOI:

Role of lattice parameter on heterogeneous ice nucleation; surface roughness of the inner wall of the three ring systems; contact angle hysteresis of the sessile water droplet on different pyroelectric single crystals; effect of cooling rate on water freezing (PDF).

References

Abe, K., Sumi, T., Koga, K., 2014. Temperature dependence of local solubility of hydrophobic molecules in the liquid-vapor interface of water. The Journal of chemical physics 141, 18C516. URL: http://dx.doi.org/10.1063/1.4896236, doi:10.1063/1.4896236.

37

Alizadeh, A., Yamada, M., Li, R., Shang, W., Otta, S., Zhong, S., Ge, L., Dhinojwala, A., Conway, K.R., Bahadur, V., Vinciquerra, A.J., Stephens, B., Blohm, M.L., 2012. Dynamics of ice nucleation on water repellent surfaces. Langmuir 28, 3180–3186. URL: `http://dx.doi.org/10.1021/la2045256`, doi:`10.1021/la2045256`.

Ashbaugh, H.S., Paulaitis, M.E., 2001. Effect of solute size and solute-water attractive interactions on hydration water structure around hydrophobic solutes. Journal of the American Chemical Society 123, 10721–10728. URL: `http://dx.doi.org/10.1021/ja016324k`, doi:`10.1021/ja016324k`. pMID: 11674005.

Bartholomäus, T., Buse, K., Deuper, C., Krätzig, E., 1994. Pyroelectric coefficients of LiNbO$_3$ crystals of different compositions. physica status solidi (a) 142, K55–K57. URL: `http://dx.doi.org/10.1002/pssa.2211420146`, doi:`10.1002/pssa.2211420146`.

Bigg, E.K., 1953. The supercooling of water. Proceedings of the Physical Society. Section B 66, 688. URL: `http://stacks.iop.org/0370-1301/66/i=8/a=309`.

Boreyko, J.B., Collier, C.P., 2013. Delayed frost growth on jumping-drop superhydrophobic surfaces. ACS Nano 7, 1618–1627. URL: `http://dx.doi.org/10.1021/nn3055048`, doi:`10.1021/nn3055048`. pMID: 23286736.

Boreyko, J.B., Hansen, R.R., Murphy, K.R., Nath, S., Retterer, S.T., Collier, C.P., 2016. Controlling condensation and frost growth with chemical

micropatterns. Scientific Reports 6. URL: `http://dx.doi.org/10.1038/srep19131`, doi:10.1038/srep19131.

Bronshteyn, V.L., Chernov, A.A., 1991. Freezing potentials arising on solidification of dilute aqueous solutions of electrolytes. Journal of Crystal Growth 112, 129 – 145. URL: `//www.sciencedirect.com/science/article/pii/002202489190918U`, doi:`http://dx.doi.org/10.1016/0022-0248(91)90918-U`.

Butt, H.J., Graf, K., Kappl, M., 2003. Physics and Chemistry of Interfaces. Wiley-VCH, Weinheim. URL: `http://onlinelibrary.wiley.com/book/10.1002/3527602313`, doi:10.1002/3527602313.

Butt, H.J., Untch, M.B., Golriz, A., Pihan, S.A., Berger, R., 2011. Electric-field-induced condensation: An extension of the Kelvin equation. Phys. Rev. E 83, 061604. URL: `http://link.aps.org/doi/10.1103/PhysRevE.83.061604`, doi:10.1103/PhysRevE.83.061604.

Carte, A.E., 1956. The freezing of water droplets. Proceedings of the Physical Society. Section B 69, 1028–1034. URL: `http://stacks.iop.org/0370-1301/69/i=10/a=309`.

Cerdeirina, C.A., Debenedetti, P.G., 2016. Water anomalous thermodynamics, attraction, repulsion, and hydrophobic hydration. The Journal of Chemical Physics 144, 164501. URL: `http://dx.doi.org/10.1063/1.4947062`, doi:10.1063/1.4947062.

Chen, L., Bonaccurso, E., 2014. Electrowetting – from statics to dynamics. Advances in Colloid and Interface Science 210, 2 –

39

12. URL: `http://www.sciencedirect.com/science/article/pii/S0001868613001140`, doi:`http://dx.doi.org/10.1016/j.cis.2013.09.007`.

Curtiss, L.A., Melendres, C.A., 1984. A theoretical study of the solvation of oxygen in water. The Journal of Physical Chemistry 88, 1325–1329. URL: `http://dx.doi.org/10.1021/j150651a018`, doi:`10.1021/j150651a018`.

Damjanovic, D., 1998. Ferroelectric, dielectric and piezoelectric properties of ferroelectric thin films and ceramics. Reports on Progress in Physics 61, 1267. URL: `http://stacks.iop.org/0034-4885/61/i=9/a=002`.

Djikaev, Y.S., Tabazadeh, A., Hamill, P., Reiss, H., 2002. Thermodynamic conditions for the surface-stimulated crystallization of atmospheric droplets. The Journal of Physical Chemistry A 106, 10247–10253. URL: `http://dx.doi.org/10.1021/jp021044s`, doi:`10.1021/jp021044s`.

Dooley, J.B., 2010. Determination and characterization of ice propagation mechanisms on surfaces undergoing dropwise condensation. dissertation. Texas A&M University.

Duft, D., Leisner, T., 2004. Laboratory evidence for volume-dominated nucleation of ice in supercooled water microdroplets. Atmospheric Chemistry and Physics 4, 1997–2000. URL: `http://www.atmos-chem-phys.net/4/1997/2004/`, doi:`10.5194/acp-4-1997-2004`.

Earle, M.E., Kuhn, T., Khalizov, A.F., Sloan, J.J., 2010. Volume nucleation rates for homogeneous freezing in supercooled water microdroplets: results from a combined experimental and mod-

40

elling approach. Atmospheric Chemistry and Physics 10, 7945–7961.
URL: `http://www.atmos-chem-phys.net/10/7945/2010/`, doi:10.5194/
`acp-10-7945-2010`.

Ehre, D., Lavert, E., Lahav, M., Lubomirsky, I., 2010. Water freezes differ-
ently on positively and negatively charged surfaces of pyroelectric materi-
als. Science 327, 672–675. URL: `http://www.sciencemag.org/content/`
`327/5966/672.abstract`, doi:10.1126/science.1178085.

Enrquez, O.R., lvaro G. Marn, Winkels, K.G., Snoeijer, J.H., 2012. Freezing
singularities in water drops. Physics of Fluids 24, 091102. URL: `https:`
`//doi.org/10.1063/1.4747185`, doi:10.1063/1.4747185.

Fan, S.K., Yang, H., Wang, T.T., Hsu, W., 2007. Asymmetric electrowetting-
moving droplets by a square wave. Lab Chip 7, 1330–1335. URL: `http:`
`//dx.doi.org/10.1039/B704084A`, doi:10.1039/B704084A.

Frank, H.S., Evans, M.W., 1945. Free volume and entropy in condensed
systems III. Entropy in binary liquid mixtures; partial molal entropy in
dilute solutions; structure and thermodynamics in aqueous electrolytes.
The Journal of Chemical Physics 13, 507–532. URL: `http://dx.doi.`
`org/10.1063/1.1723985`, doi:10.1063/1.1723985.

Frankenstein, S., Tuthill, A.M., 2002. Ice adhesion to locks and dams: Past
work; future directions? Journal of Cold Regions Engineering 16, 83–96.
URL: `http://dx.doi.org/10.1061/(ASCE)0887-381X(2002)16:2(83)`,
doi:10.1061/(ASCE)0887-381X(2002)16:2(83).

41

Gao, G.T., Oh, K.J., Zeng, X.C., 1999. Effect of uniform electric field on homogeneous vapor-liquid nucleation and phase equilibria. II. Extended simple point charge model water. The Journal of Chemical Physics 110, 2533–2538. URL: `http://dx.doi.org/10.1063/1.477959`, doi:10.1063/1.477959.

Glass, A.M., 1969. Investigation of the electrical properties of $Sr_{1-x}Ba_xNb_2O_6$ with special reference to pyroelectric detection. Journal of Applied Physics 40, 4699–4713. URL: `http://scitation.aip.org/content/aip/journal/jap/40/12/10.1063/1.1657277`, doi:`http://dx.doi.org/10.1063/1.1657277`.

Guadarrama-Cetina, J., Mongruel, A., González-Vinas, W., Beysens, D., 2013. Percolation-induced frost formation. EPL (Europhysics Letters) 101, 16009. URL: `http://stacks.iop.org/0295-5075/101/i=1/a=16009`.

Guillot, B., Guissani, Y., 1993. A computer simulation study of the temperature dependence of the hydrophobic hydration. The Journal of Chemical Physics 99, 8075–8094. URL: `http://dx.doi.org/10.1063/1.465634`, doi:10.1063/1.465634.

Hayon, E., 1962. Role of oxygen in the primary formation of H and H_2O^- in the radiation chemistry of water. Nature 196, 533–534. URL: `http://dx.doi.org/10.1038/196533a0`, doi:10.1038/196533a0.

Heidt, L.J., Ekstrom, L., 1957. Influence of dissolved air on optical density measurements of water solutions. Journal of the American Chemical So-

ciety 79, 1260–1261. URL: http://dx.doi.org/10.1021/ja01562a061,
doi:10.1021/ja01562a061.

Heidt, L.J., Johnson, A.M., 1957. Optical study of the hydrates of molecular
oxygen in water. Journal of the American Chemical Society 79, 5587–
5593. URL: http://dx.doi.org/10.1021/ja01578a001, doi:10.1021/
ja01578a001.

Hoffer, T.E., 1961. A laboratory investigation of droplet freez-
ing. Journal of Meteorology 18, 766–778. URL: http://dx.
doi.org/10.1175/1520-0469(1961)018<0766:ALIODF>2.0.CO;2,
doi:10.1175/1520-0469(1961)018<0766:ALIODF>2.0.CO;2.

Huang, L., Liu, Z., Liu, Y., Gou, Y., Wang, L., 2012. Effect of contact
angle on water droplet freezing process on a cold flat surface. Ex-
perimental Thermal and Fluid Science 40, 74 – 80. URL: http://
www.sciencedirect.com/science/article/pii/S0894177712000477,
doi:http://dx.doi.org/10.1016/j.expthermflusci.2012.02.002.

Ishikawa, Y., Shiozawa, M., Kondo, M., Ito, K., 2014. Theoretical
analysis of supercooled states of water generated below the freezing
point in a PEFC. International Journal of Heat and Mass Trans-
fer 74, 215 – 227. URL: http://www.sciencedirect.com/science/
article/pii/S0017931014002440, doi:http://dx.doi.org/10.1016/j.
ijheatmasstransfer.2014.03.038.

Johnson, N.L., Kotz, S., Balakrishnan, N., 1994. Continuous Univariate

43

Distributions, Volume 1 (Wiley Series in Probability and Mathematical Statistics). 2nd ed., Wiley-Interscience.

Joshi, J.C., Dawar, A.L., 1982. Pyroelectric materials, their properties and applications. physica status solidi (a) 70, 353–369. URL: http://dx.doi.org/10.1002/pssa.2210700202, doi:10.1002/pssa.2210700202.

Jung, S., Tiwari, M.K., Doan, N.V., Poulikakos, D., 2012. Mechanism of supercooled droplet freezing on surfaces. Nature Communications 3, 615. URL: http://dx.doi.org/10.1038/ncomms1630, doi:10.1038/ncomms1630.

Kashchiev, D., Firoozabadi, A., 2002. Nucleation of gas hydrates. Journal of Crystal Growth 243, 476 – 489. URL: http://www.sciencedirect.com/science/article/pii/S0022024802015762, doi:http://dx.doi.org/10.1016/S0022-0248(02)01576-2.

Kletetschka, G., Hruba, J., 2015. Dissolved gases and ice fracturing during the freezing of a multicellular organism: Lessons from tardigrades. BioResearch Open Access 4, 209–217. URL: http://dx.doi.org/10.1089/biores.2015.0008, doi:10.1089/biores.2015.0008.

Knopf, D.A., Alpert, P.A., 2013. A water activity based model of heterogeneous ice nucleation kinetics for freezing of water and aqueous solution droplets. Faraday Discuss. 165, 513–534. URL: http://dx.doi.org/10.1039/C3FD00035D, doi:10.1039/C3FD00035D.

Koga, K., 2011. Solvation of hydrophobes in water and simple liquids.

44

Physical Chemistry Chemical Physics 13, 19749–19758. URL: `http://dx.doi.org/10.1039/C1CP22344E`, doi:10.1039/C1CP22344E.

Koo, B., Kim, C.J., 2013. Evaluation of repeated electrowetting on three different fluoropolymer top coatings. Journal of Micromechanics and Microengineering 23, 067002. URL: `http://stacks.iop.org/0960-1317/23/i=6/a=067002`.

Kreder, M.J., Alvarenga, J., Kim, P., Aizenberg, J., 2016. Design of anti-icing surfaces: smooth, textured or slippery? Nature Reviews Materials 1, 15003. URL: `http://dx.doi.org/10.1038/natrevmats.2015.3`.

Kuhn, T., Earle, M.E., Khalizov, A.F., Sloan, J.J., 2011. Size dependence of volume and surface nucleation rates for homogeneous freezing of supercooled water droplets. Atmospheric Chemistry and Physics 11, 2853–2861. URL: `http://www.atmos-chem-phys.net/11/2853/2011/`, doi:10.5194/acp-11-2853-2011.

Laforte, J., Allaire, M., Laflamme, J., 1998. State-of-the-art on power line de-icing. Atmospheric Research 46, 143 – 158. URL: `http://www.sciencedirect.com/science/article/pii/S0169809597000574`, doi:10.1016/S0169-8095(97)00057-4.

Lang, S.B., 2005. Pyroelectricity: From ancient curiosity to modern imaging tool. Physics Today 58, 31–36. URL: `http://scitation.aip.org/content/aip/magazine/physicstoday/article/58/8/10.1063/1.2062916`, doi:http://dx.doi.org/10.1063/1.2062916.

45

Langham, E.J., Mason, B.J., 1958. The heterogeneous and homogeneous nucleation of supercooled water. Proceedings of the Royal Society of London A: Mathematical, Physical and Engineering Sciences 247, 493–504. URL: `http://rspa.royalsocietypublishing.org/content/247/1251/493`, doi:10.1098/`rspa.1958.0207`.

Li, K., Xu, S., Shi, W., He, M., Li, H., Li, S., Zhou, X., Wang, J., Song, Y., 2012. Investigating the effects of solid surfaces on ice nucleation. Langmuir 28, 10749–10754. URL: `http://dx.doi.org/10.1021/la3014915`, doi:10.1021/`la3014915`. pMID: 22741592.

Marín, A.G., Enríquez, O.R., Brunet, P., Colinet, P., Snoeijer, J.H., 2014. Universality of tip singularity formation in freezing water drops. Phys. Rev. Lett. 113, 054301. URL: `https://link.aps.org/doi/10.1103/PhysRevLett.113.054301`, doi:10.1103/`PhysRevLett.113.054301`.

Meakin, P., 1992. Dropwise condensation: the deposition growth and coalescence of fluid droplets. Physica Scripta 1992, 31. URL: `http://stacks.iop.org/1402-4896/1992/i=T44/a=004`.

Miljkovic, N., Preston, D.J., Enright, R., Wang, E.N., 2013. Electrostatic charging of jumping droplets. Nature Communications 4, 2517. URL: `http://dx.doi.org/10.1038/ncomms3517`, doi:10.1038/`ncomms3517`.

Mishchenko, L., Hatton, B., Bahadur, V., Taylor, J.A., Krupenkin, T., Aizenberg, J., 2010. Design of ice-free nanostructured surfaces based on repulsion of impacting water droplets. ACS Nano 4, 7699–7707. URL: `http://dx.doi.org/10.1021/nn102557p`, doi:10.1021/`nn102557p`.

Moon, H., Cho, S.K., Garrell, R.L., Kim, C.J.., 2002. Low voltage electrowetting-on-dielectric. Journal of Applied Physics 92, 4080–4087. URL: `http://dx.doi.org/10.1063/1.1504171`, doi:10.1063/1.1504171.

Murray, C., Riley, J., 1969. The solubility of gases in distilled water and sea water – II. Oxygen. Deep Sea Research and Oceanographic Abstracts 16, 311 – 320. URL: `http://www.sciencedirect.com/science/article/pii/0011747169900217`, doi:`http://dx.doi.org/10.1016/0011-7471(69)90021-7`.

Na, B., Webb, R.L., 2003. A fundamental understanding of factors affecting frost nucleation. International Journal of Heat and Mass Transfer 46, 3797 – 3808. URL: `http://www.sciencedirect.com/science/article/pii/S0017931003001947`, doi:`http://dx.doi.org/10.1016/S0017-9310(03)00194-7`.

Newnham, R.E., 2005. Properties of Materials: Anisotropy, Symmetry, Structure. Oxford University Press, New York.

Ning, D., Liu, X.Y., 2002. Controlled ice nucleation in microsized water droplet. Applied Physics Letters 81, 445–447. URL: `http://scitation.aip.org/content/aip/journal/apl/81/3/10.1063/1.1492849`, doi:`http://dx.doi.org/10.1063/1.1492849`.

Nitsch, K., 2009. Thermal analysis study on water freezing and supercooling. Journal of Thermal Analysis and Calorimetry 95, 11–14.

47

URL: `http://dx.doi.org/10.1007/s10973-008-9074-8`, doi:`10.1007/s10973-008-9074-8`.

O, K.T., Wood, R., 2016. Exploring an approximation for the homogeneous freezing temperature of water droplets. Atmospheric Chemistry and Physics 16, 7239–7249. URL: `http://www.atmos-chem-phys.net/16/7239/2016/`, doi:`10.5194/acp-16-7239-2016`.

Oberli, L., Caruso, D., Hall, C., Fabretto, M., Murphy, P.J., Evans, D., 2014. Condensation and freezing of droplets on superhydrophobic surfaces. Advances in Colloid and Interface Science 210, 47 – 57. URL: `http://www.sciencedirect.com/science/article/pii/S0001868613001334`, doi:`http://dx.doi.org/10.1016/j.cis.2013.10.018`. thin liquid films in wetting, spreading and surface interactions: a collection of papers presented at 6th Australian Colloid & Interface Symposium.

O'Concubhair, R., Sodeau, J.R., 2013. The effect of freezing on reactions with environmental impact. Accounts of Chemical Research 46, 2716–2724. URL: `http://dx.doi.org/10.1021/ar400114e`, doi:`10.1021/ar400114e`. pMID: 23829881.

Oleinikova, A., Brovchenko, I., 2012. Thermodynamic properties of hydration water around solutes: Effect of solute size and watersolute interaction. The Journal of Physical Chemistry B 116, 14650–14659. URL: `http://dx.doi.org/10.1021/jp306781y`, doi:`10.1021/jp306781y`. pMID: 23171283.

O'Neill, M.J., 1964. The analysis of a temperature-controlled scanning

48

calorimeter. Analytical Chemistry 36, 1238–1245. URL: `http://dx.doi.org/10.1021/ac60213a020`, doi:10.1021/ac60213a020.

Parody-Morreale, A., Bishop, G., Fall, R., Gill, S.J., 1986. A differential scanning calorimeter for ice nucleation distribution studiesapplication to bacterial nucleators. Analytical Biochemistry 154, 682 – 690. URL: `http://www.sciencedirect.com/science/article/pii/0003269786900473`, doi:http://dx.doi.org/10.1016/0003-2697(86)90047-3.

Parungo, F.P., Lodge, J.P., 1967. Freezing of aqueous solutions of non-polar gases. Journal of the Atmospheric Sciences 24, 439–441. URL: `http://dx.doi.org/10.1175/1520-0469(1967)024<0439:FOASON>2.0.CO;2`, doi:10.1175/1520-0469(1967)024<0439:FOASON>2.0.CO;2.

Petit, J., Bonaccurso, E., 2014. General frost growth mechanism on solid substrates with different stiffness. Langmuir 30, 1160–1168. URL: `http://dx.doi.org/10.1021/la404084m`, doi:10.1021/la404084m. pMID: 24456462.

Ping, S.S., Lin, L.H., 1981. Dielectric and pyroelectric properties of $LiTaO_3$ single crystals. Ferroelectrics 38, 821–823. URL: `http://dx.doi.org/10.1080/00150198108209548`, doi:10.1080/00150198108209548.

Pruppacher, H.R., Klett, J.D., 1978. Microphysics of Clouds and Precipitation. Springer Netherlands. doi:10.1007/978-94-009-9905-3.

Putley, E., 1980. The possibility of background limited pyroelectric detectors. Infrared Physics 20, 149 – 156. URL: `http://www.sciencedirect.com/`

science/article/pii/0020089180900214, doi:http://dx.doi.org/10.
1016/0020-0891(80)90021-4.

Rettich, T., Battino, R., Wilhelm, E., 2000. Solubility of gases
in liquids. 22. High-precision determination of Henry's law con-
stants of oxygen in liquid water from $T = 274$ K to $T = 328$ K. The Journal of Chemical Thermodynamics 32, 1145
– 1156. URL: http://www.sciencedirect.com/science/article/
pii/S0021961499905815, doi:http://dx.doi.org/10.1006/jcht.1999.
0581.

Ristenpart, W.D., Bird, J.C., Belmonte, A., Dollar, F., Stone, H.A., 2009.
Non-coalescence of oppositely charged drops. Nature 461, 377–380. URL:
http://dx.doi.org/10.1038/nature08294, doi:10.1038/nature08294.

Saito, H., Takai, K., Yamauchi, G., 1997. Water- and ice-repellent coatings.
Surface Coatings International 80, 168–171. URL: http://dx.doi.org/
10.1007/BF02692637, doi:10.1007/BF02692637.

Scheraga, H.A., 1965. The effect of solutes on the structure of wa-
ter and its implications for protein structure*. Annals of the New
York Academy of Sciences 125, 253–276. URL: http://dx.doi.org/10.
1111/j.1749-6632.1965.tb45396.x, doi:10.1111/j.1749-6632.1965.
tb45396.x.

Schetnikov, A., Matiunin, V., Chernov, V., 2015. Conical shape of frozen
water droplets. American Journal of Physics 83, 36–38. URL: https:
//doi.org/10.1119/1.4897499, doi:10.1119/1.4897499.

50

Schutzius, T.M., Jung, S., Maitra, T., Eberle, P., Antonini, C., Stamatopoulos, C., Poulikakos, D., 2015. Physics of icing and rational design of surfaces with extraordinary icephobicity. Langmuir 31, 4807–4821. URL: http://dx.doi.org/10.1021/la502586a, doi:10.1021/la502586a. pMID: 25346213.

Seeley, L.H., Seidler, G.T., 2001. Preactivation in the nucleation of ice by Langmuir films of aliphatic alcohols. The Journal of Chemical Physics 114, 10464–10470. URL: http://dx.doi.org/10.1063/1.1375151, doi:10.1063/1.1375151.

Shapiro, B., Moon, H., Garrell, R.L., Kim, C.J.., 2003. Equilibrium behavior of sessile drops under surface tension, applied external fields, and material variations. Journal of Applied Physics 93, 5794–5811. URL: http://dx.doi.org/10.1063/1.1563828, doi:10.1063/1.1563828.

Shaw, R.A., Durant, A.J., Mi, Y., 2005. Heterogeneous surface crystallization observed in undercooled water. The Journal of Physical Chemistry B 109, 9865–9868. URL: http://dx.doi.org/10.1021/jp0506336, doi:10.1021/jp0506336. pMID: 16852192.

Singh, D.P., Singh, J.P., 2013. Delayed freezing of water droplet on silver nanocolumnar thin film. Applied Physics Letters 102, 243112. URL: http://dx.doi.org/10.1063/1.4811751, doi:10.1063/1.4811751.

Snoeijer, J.H., Brunet, P., 2012. Pointy ice-drops: How water freezes into a singular shape. American Journal of Physics 80, 764–771. URL: http://dx.doi.org/10.1119/1.4726201, doi:10.1119/1.4726201.

51

Spitzner, D., Bergmann, U., Apelt, S., Boucher, R.A., Wiesmann, H.P., 2015. Reversible switching of icing properties on pyroelectric polyvenylidene fluoride thin film coatings. Coatings 5, 724–736. URL: `http://www.mdpi.com/2079-6412/5/4/724`, doi:10.3390/coatings5040724.

Sun, Y., Huang, X., Soh, S., 2016. Solid-to-liquid charge transfer for generating droplets with tunable charge. Angewandte Chemie International Edition 55, 9956–9960. URL: `http://dx.doi.org/10.1002/anie.201604378`, doi:10.1002/anie.201604378.

Tabazadeh, A., Djikaev, Y.S., Reiss, H., 2002. Surface crystallization of supercooled water in clouds. Proceedings of the National Academy of Sciences 99, 15873–15878. URL: `http://www.pnas.org/content/99/25/15873.abstract`, doi:10.1073/pnas.252640699.

Takenaka, N., Bandow, H., 2007. Chemical kinetics of reactions in the unfrozen solution of ice. The Journal of Physical Chemistry A 111, 8780–8786. URL: `http://dx.doi.org/10.1021/jp0738356`, doi:10.1021/jp0738356. pMID: 17705357.

Wang, J., Liu, Z., Gou, Y., Zhang, X., Cheng, S., 2006. Deformation of freezing water droplets on a cold copper surface. Science in China Series E: Technological Sciences 49, 590–600. URL: `http://dx.doi.org/10.1007/s11431-006-2017-y`, doi:10.1007/s11431-006-2017-y.

Weibull, W., 1951. A statistical distribution function of wide applicability. Journal of Applied Mechanics 18, 293–297.

52

Weiss, R., 1970. The solubility of nitrogen, oxygen and argon in water and seawater. Deep Sea Research and Oceanographic Abstracts 17, 721 – 735. URL: `http://www.sciencedirect.com/science/article/pii/0011747170900379`, doi:`http://dx.doi.org/10.1016/0011-7471(70)90037-9`.

Wilson, P., Heneghan, A., Haymet, A., 2003. Ice nucleation in nature: supercooling point (SCP) measurements and the role of heterogeneous nucleation. Cryobiology 46, 88 – 98. URL: `http://www.sciencedirect.com/science/article/pii/S0011224002001827`, doi:`http://dx.doi.org/10.1016/S0011-2240(02)00182-7`.

Wilson, P.W., Haymet, A.D.J., 2012. The spread of nucleation temperatures of a sample of supercooled liquid is independent of the average nucleation temperature. The Journal of Physical Chemistry B 116, 13472–13475. URL: `http://dx.doi.org/10.1021/jp308177b`, doi:`10.1021/jp308177b`. pMID: 23102116.

Wojciechowski, B., Owczarek, I., Bednarz, G., 1988. Freezing of aqueous solutions containing gases. Crystal Research and Technology 23, 843–848. URL: `http://dx.doi.org/10.1002/crat.2170230702`, doi:`10.1002/crat.2170230702`.

Wood, G.R., Walton, A.G., 1970. Homogeneous nucleation kinetics of ice from water. Journal of Applied Physics 41, 3027–3036. URL: `http://dx.doi.org/10.1063/1.1659359`, doi:`10.1063/1.1659359`.

Workman, E.J., Reynolds, S.E., 1950. Electrical phenomena occurring during

the freezing of dilute aqueous solutions and their possible relationship to thunderstorm electricity. Phys. Rev. 78, 254–259. URL: `http://link.aps.org/doi/10.1103/PhysRev.78.254`, doi:10.1103/PhysRev.78.254.

Yokota, M., Okumura, K., 2011. Dimensional crossover in the coalescence dynamics of viscous drops confined in between two plates. Proceedings of the National Academy of Sciences 108, 6395–6398. URL: `http://www.pnas.org/content/108/16/6395.abstract`, doi:10.1073/pnas.1017112108.

Zhang, Y., Anim-Danso, E., Bekele, S., Dhinojwala, A., 2016. Effect of surface energy on freezing temperature of water. ACS Applied Materials & Interfaces 8, 17583–17590. URL: `http://dx.doi.org/10.1021/acsami.6b02094`, doi:10.1021/acsami.6b02094. pMID: 27314147.

Zobrist, B., Koop, T., Luo, B.P., Marcolli, C., Peter, T., 2007. Heterogeneous ice nucleation rate coefficient of water droplets coated by a nonadecanol monolayer. The Journal of Physical Chemistry C 111, 2149–2155. URL: `http://dx.doi.org/10.1021/jp066080w`, doi:10.1021/jp066080w.

Graphical Abstract
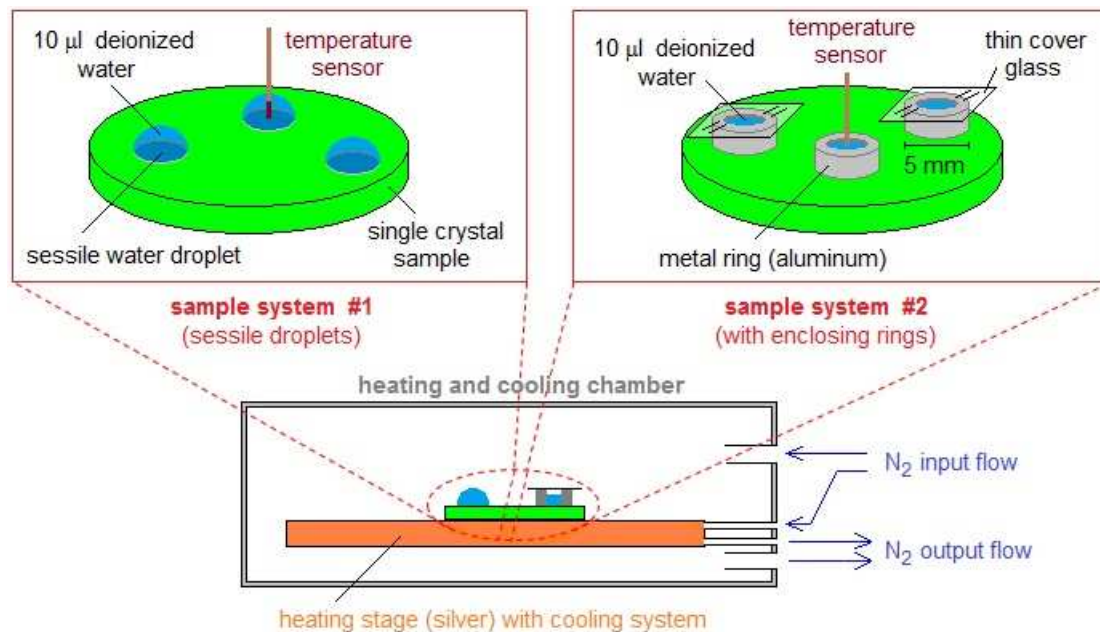
Highlights

- Two measurement setups were used in order to determine the icing temperatures of small water droplets on different pyroelectric single crystals

- The degree of supercooling was found to vary between different pyroelectric single crystals

- A possible correlation between the pyroelectric coefficient and icing temperature was found only within a certain range of the coefficient

- Different experimental methods lead to measurable differences in the icing temperature due to various external in uence factors

56